Image-based Road Marking Classification and Vector Data Derivation from Mobile Mapping 3D Point Clouds

Johannes Wolf, Tobias Pietz, Rico Richter, Sören Discher and Jürgen Döllner
Hasso Plattner Institute, Faculty of Digital Engineering, University of Potsdam, Germany

Keywords: GIS, LiDAR, Point Cloud Rendering, Digital Image Analysis.

Abstract: Capturing urban areas and infrastructure for automated analysis processes becomes ever more important. Laserscanning and photogrammetry are used for scanning the environment in highly detailed resolution. In this work, we present techniques for the semantic classification of 3D point clouds from mobile mapping scans of road environments and the detection of road markings. The approach renders 3D point cloud input data into images for which U-Net as an established image recognition convolutional neural network is used for the semantic classification. The results of the classification are projected back into the 3D point cloud. An automated extraction of vector data is applied for detected road markings, generating detailed road marking maps. Different approaches for the vector data generation are used depending on the type of road markings, such as arrows or dashed lines. The automatically generated shape files created by the presented process can be further used in various GIS applications. Our results of the implemented out-of-core techniques show that the approach can efficiently be applied on large datasets of entire cities.

1 INTRODUCTION

In recent years, 3D point clouds have established themselves as a common data format for acquired geospatial data. They offer the possibility of easy and direct data acquisition and can contain very detailed information about the scanned environment (Vosselman et al., 2004). They are a discrete representation of the real world and can be used for any environment without the need for specific configuration (Haala et al., 2008). 3D point clouds can be updated with low effort and are well-suited for an automated analysis. Individual points are stored without semantic order and can be provided with any attributes in addition to their three-dimensional coordinates. For example, LiDAR scans contain additional intensity values (Richter et al., 2013). Due to the lack of order and structure, measuring points only offer added value when they are viewed together in semantic units. Therefore, a semantic classification is usually performed before further use of the data (Niemeyer et al., 2012). Semantic classification describes the process of assigning individual points a semantic class that describes to which type of object the point belongs, for example “Roadway”, “Traffic sign”, or “Vehicle”. Once semantic information is available, further analyses can be performed on the 3D point clouds. For example, they can be used to create or update street cadastres (Caroti et al., 2005) or to check that light spaces are kept free (Mikrut et al., 2016). The basis for semantic classification is usually a differentiation between basic classes such as ground, vegetation, and buildings, but the analysis can be as detailed as required and, depending on the application, include classes such as curbs, road markings, or traffic signs (Pu et al., 2011).

Current information about the condition of traffic infrastructure is of great interest to municipalities and traffic offices. Road markings are essential for the regulation of traffic flow, especially in crossing situations. When planning construction sites and after the recreation of the previous state after road works, road construction offices require detailed information about the location of road markings. In everyday applications, navigation systems use a map with information about the number of lanes and which lane must be used to turn into a certain direction (Bétaille and Toledo-Moreo, 2010). For autonomous driving, cars need to continuously detect road markings to keep the car in its lane and use a base map with lane information for anticipating the course (Maurer et al., 2016).

Thus, there is a need for efficiently capturing information about road markings and the automated

Wolf, J., Pietz, T., Richter, R., Discher, S. and Döllner, J.
Image-based Road Marking Classification and Vector Data Derivation from Mobile Mapping 3D Point Clouds.
DOI: 10.5220/0010190602270234
In *Proceedings of the 16th International Joint Conference on Computer Vision, Imaging and Computer Graphics Theory and Applications (VISIGRAPP 2021) - Volume 4: VISAPP*, pages 227-234
ISBN: 978-989-758-488-6

creation of detailed road maps. Mobile mapping scans are an established data source for the required information, 3D point clouds being measured via LiDAR include valuable intensity data for the localization of road markings and they can easily be captured in urban regions. The intensity value represents the strength of the reflection of the scanning laser, enabling conclusions about the structure of the surface or its material. As shown in Figures 2 and 4, road markings by design have a much higher intensity value than the surrounding pavement.

In this work, we focus on a semantic classification of road markings using convolutional neural networks (CNNs) for visual recognition in images. Convolutional neural networks are a class of networks used in machine learning that were inspired by biological processes and find use especially in the automated analysis of image data (LeCun et al., 2010).

Automated image analysis has been an active field of research for many years and popular frameworks have been developed that can be used for own use cases (Pulli et al., 2012). Some objects in 3D point clouds are particularly suitable for a classification based on image analysis as we have shown before (Wolf et al., 2019a). Here we present a complete process for the analysis and vector data derivation of road markings in 3D point clouds for which these approaches can be used if the input data are processed and rendered in a suitable way.

2 RELATED WORK

3D point clouds commonly serve as base data to automatically derive 3D city models and landscape models (Schwalbe et al., 2005) for many different use cases in urban planning for local authorities, companies, or individuals (Vosselman et al., 2001). As showcased by several existing tools, cadastral data can be visualized in combination with 3D point clouds to provide additional context and further facilitate the visual analysis and task-oriented exploration of captured data sets (Aringer and Roschlaub, 2014). High density point information can be analyzed and creating large models gets possible, requiring only minimal manual effort (Richter and Döllner, 2013). Besides aerial captures of 3D point clouds, mobile mapping techniques are widely used (Li, 1997). Mobile mapping scans can be used to, e. g., automatically extract road networks, or to analyze road surfaces (Jaakkola et al., 2008), as well as for the reconstruction of building facades.

For many use cases the automated semantic analysis of 3D point clouds is a mandatory preparation. Examples include ground detection, tree analysis, change detection between multiple scans, cadastre comparison, or automated 3D model generation. Semantic classification can be performed by two fundamentally different approaches: Semantic per-point surface category information can be derived by analyzing a 3D point cloud's topology (Chen et al., 2017) or by applying deep learning concepts (Boulch et al., 2017).

In a more traditional approach, geometric attributes are evaluated to determine the respective class of individual points and of point groups (Grilli et al., 2017). 3D point clouds can be divided into local groups, so-called segments, for example by grouping points with similar surface orientation (Rabbani et al., 2006). The resulting segments can then be analyzed individually. The size and orientation of the included surfaces are considered. Thus, large vertical surfaces can usually be recognized as building facades, whereas point groups with strongly varying surface normals typically indicate vegetation (Wolf et al., 2019b).

In recent years procedures have been established as an alternative that practice classification by means of machine learning (Zhou and Tuzel, 2018). For this purpose, artificial neural networks are trained using already classified data to be able to make statements about the probable semantic class of points in unknown 3D point clouds. It also became popular to use the internal structures of the 3D point cloud itself for prediction, as in the case of PointNet and similar networks (Qi et al., 2017). However, these approaches often use small data sets of individual objects and require comprehensive training data.

Detecting objects in image data is a relevant research field for many applications, such as face recognition, license plate identification, or medical imagery analysis. Viola et al. (2001) present an image object detection algorithm which can be used to detect, e. g., faces in images.

U-Net, which was originally developed for the medical sector, is now widely used in image segmentation (Ronneberger et al., 2015). With the help of this network, specific areas in images can be recognized, such as cancer cells but also streets in aerial images (Zhang et al., 2018).

The extraction of road marking information from images taken from a car is discussed by Vacek et al. (2007), who detect lanes and arrow markings. Veit et al. (2008) present an approach to evaluate the performance of algorithms for the road marking detection in images in general.

Yang et al. (2012) use the reflective properties of road markings to extract them from LiDAR 3D point

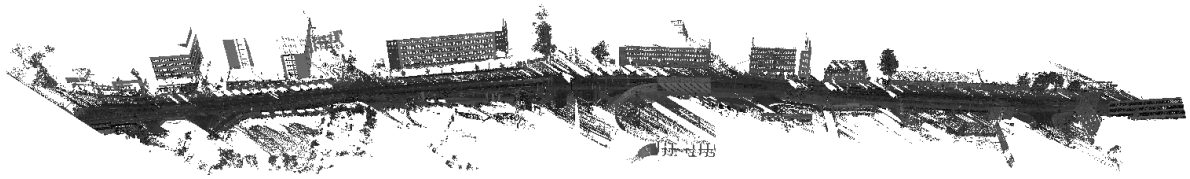

Figure 1: 3D point cloud of a street used as input for the road marking detection.

Table 1: Data used for training.

City	No. scans	Approx. area covered	No. rendered images	Details
Essen	2	4 720 m^2	233	A straight road with 62 road markings and a crossing with 351 road markings.
Hamburg	2	7 610 m^2	376	Two large crossings with 1537 road markings in total.
Potsdam	0	—	—	No ground truth data was available, so this dataset was not used for training.

Table 2: Data used for manual evaluation.

City	No. scans	Approx. area covered	No. rendered images	Details
Essen	1	2 980 m^2	147	Straight road with T-junction at the end.
Hamburg	1	5 510 m^2	272	Large crossing with multiple lanes (shown in Figure 7).
Potsdam	1	2 150 m^2	106	Small 4-way crossing.

clouds. Similarly, Guan et al. (2014) present how mobile laser scanning data can be used for an extraction of road markings. They perform a curb-based road extraction, followed by rendering intensity images of the 3D point cloud and a final extraction step, segmenting the areas containing road markings. Yu et al. (2014) take this approach one step further by distinguishing seven specific types of road markings by five classification methods.

Figure 2: 3D point cloud of a crossing with road markings. Detail of the 3D point cloud shown in Figure 1. Intensity values are represented in grayscale, lighter colors have higher intensity values.

3 DATASETS

The datasets used in this work are mobile mapping scans from three different cities in Germany. They vary with respect to point densities and the number of cars, pedestrians, and other objects blocking the view. However, the trained network can detect road markings in all datasets with similar accuracy. Different areas of the datasets were used for training and evaluation, as presented in Table 1 and Table 2. A typical street from a dataset is shown in Figure 1 and in more detail in Figure 2. The 3D point cloud shown consists of 29 million points and covers about 670 meters road with several crossings.

To create a training set for a U-Net-based neural network that is able to detect road markings, more than one thousand road markings in about 600 images have been marked using existing manually created shape files as ground truth data.

4 CONCEPT AND IMPLEMENTATION

Our approach uses the abilities of image object detection algorithms to automatically classify road markings in 3D point clouds. The road markings are clearly visible in a top-down view of the 3D point cloud data. In Figure 3 the detected markings are highlighted.

The software described in this paper uses a pipeline concept for the automated processing of large data sets. First, images are rendered in which road markings are then recognized and the results of the recognition are finally transferred back to the original 3D point cloud.

Afterwards, shapes are created for individual markings. The resulting shape file can be used for

Figure 3: 3D point cloud with detected road markings represented as orange shapes rendered on top of the 3D point cloud.

further processing in GIS applications.

First, all input 3D point clouds are filtered as described in Section 4.1. Second, a renderer creates square images of these filtered 3D point clouds as described in Section 4.2.

Third, the rendered images are classified using the previously trained neural networks and the results are mapped back into the 3D point cloud, which is described in Section 4.3. Finally, Section 5 describes the creation of vector data for the individual markings.

4.1 3D Point Cloud Preprocessing

The recognition of road markings should be possible for large data sets of entire cities with billions of points. For this reason, it is important to apply appropriate data reduction. This includes first of all that only points of the street region have to be analyzed. During the acquisition of 3D point clouds, a trajectory is often captured that indicates the traveled measurement path. The resulting 3D point cloud can be clipped along this trajectory, for example, only 10 meters to the left and right along the trajectory are considered. If there is no trajectory, it can be determined approximately from the local point density, because a higher point density is recorded in areas in the immediate vicinity of the scan vehicle than in areas further away.

In the remaining data, outliers are removed by outlier filtering techniques. This is done to remove noise within the data that might affect the top-down rendering of the 3D point cloud. All points with less than, e. g., five neighboring points within a proximity of 0.5 meters can be marked as outliers. The approach can be sped up by using a heuristic search based on a spatial data structure such as a three-dimensional grid in which all points are placed. All points in cells which hold less than a certain number of points can be marked as outliers. For the specific use case of this work such a heuristic approach is sufficient because the objects of interest are all located in dense areas of the 3D point cloud.

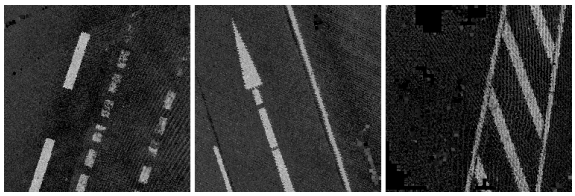

Figure 4: Examples of rendered images from a 3D point cloud, showing different types of road markings. Intensity values are represented in grayscale, lighter colors have higher intensity values.

To remove points that are too high above the road to be considered, a ground detection according to the method of Meng et al. (2009) is performed. High lying points, e. g., from surrounding buildings, or vegetation, can be removed afterwards.

The algorithm divides the area that is to be analyzed into a regular two-dimensional grid. For each grid cell, the lowest of all z-values of the points falling into this cell, is stored. This represents a simplified terrain model. After the grid has been initialized, scan lines are used to find all ground points of the 3D point cloud. These scan lines move axis-aligned in positive and negative direction as well as diagonally through the grid. The algorithm considers, which slope is determined in the different scanning directions and how the elevation differs between points and the minimum elevation in their local neighborhood. For each scan line, potential ground points are determined separately. Following that, a majority voting is used to classify points as ground.

The remaining 3D point cloud only consists of ground points along the measuring vehicle's trajectory without outliers. Following this preprocessing step, 3D point clouds of our test dataset have on average about 60 % of their original points left.

4.2 Image Rendering

After the preprocessing, images are rendered for the image analysis. Top-down views of the 3D point cloud are generated, which are processed one after the other.

The renderer receives a 3D point cloud as input and generates images of 128 by 128 pixels in orthogonal projection, as shown in Figure 4. Each image represents about 4.5 by 4.5 meters of road surface. The images are generated slightly overlapping and cover the entire area to be analyzed. By removing higher points in the preprocessing step, overhanging vegetation is removed and the road surface can be completely displayed.

Each image contains a channel with the intensity value at the respective position and a channel containing the ID of the top-most point rendered at this pixel. With this information the classification result can be transferred back to the 3D point cloud after analysis.

For best results, the points from the 3D point cloud are rendered using a rendering technique that fills holes between neighboring points (e. g., paraboloids) (Schütz and Wimmer, 2015). Rendering with different point primitives is shown in Figure 5. Using paraboloids will fill more pixels in areas with lower density to avoid holes in the resulting image, while preserving sharp edges of individual structures, as shown in Figure 5c.

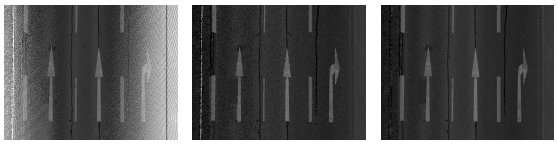

(a) Small points. (b) Large points. (c) Paraboloids.

Figure 5: 3D point cloud rendered with different primitives.

4.3 Classification

The rendered images are used as input for the previously trained neural network, working similar to the one described by Wen et al. (2019). The result is an output mask for each input image in which a semantic ID describes for each pixel, whether it represents background (road) or a certain type of road marking.

After the semantic classification of road markings by U-Net, the information about the semantic class of individual pixels can be transferred back to the 3D point cloud through the point ID channel. The point within the 3D point cloud whose ID matches that in this channel of the image is assigned the recognized semantic class as an additional attribute. The point density is generally higher than the resolution of the rendered images. Therefore, several points are covered by one pixel, so that all points in the immediate neighborhood of the point just classified also receive its semantic class, without having been noted in the ID channel itself.

5 VECTOR DATA GENERATION

Shape files are used to describe vector-based geospatial data. They can contain different types of shapes, such as points (positional data) and polygons (areal data) (ESRI, 1998). Each shape can have arbitrary attribute-value pairs, describing additional information available for this specific shape.

The presented approach creates polygonal shapes for all detected road markings, showing their precise location, size, and orientation. Each shape gets an additional attribute describing the semantic class of the road marking in this position, which can then be used for, e. g., coloring all road marking types with different colors.

Each group of adjacent points of the same semantic class will be sorted into a cluster of points to create a shape that represents the area covered by these points, resulting in shapes for road markings as shown in Figure 3. Depending of the type of road marking, different approaches for the shape creation are used, as explained below.

The resulting files can be used in various GIS applications for subsequent tasks. Figure 7 shows the rendering of an automatically created shape file.

5.1 Rectangular Lines

When creating convex hulls for rectangular road markings, these often have rough edges, resulting in a noisy visualization. A better approach is therefore the representation via oriented rectangles, concerning width, height, and orientation of the road marking.

The orientation of a line is calculated by a principal component analysis (PCA) on all points of the line, resulting in a vector describing the main direction of the points in the cluster of this line.

For each of the generated rectangles, an error value is calculated, describing which percentage of the area covered by this rectangle is not actually located on top of detected points of the road marking. Should this value get too high, the rectangle does not fit, which might occur if parts of the marking are missing or several lines are merging. In this case, an outline will be computed as described in Section 5.3.

Figure 6 shows that the orientation of the lines can be hard to determine, especially in situations where lines are not fully visible due to, e. g., abrasion.

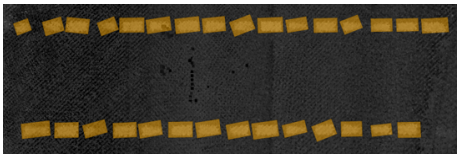

Figure 6: Example for generated polygons (orange) using individually oriented rectangles for line markings placed on top of the 3D point cloud.

To create shapes for lines consisting of individual parts, where neighboring line segments should have the same orientation, larger clusters are created. Lines from the same type are collected into a combined cluster, if the distance to the next neighboring

line is smaller than a given threshold and the orientation does only differ by a small amount. This prevents taking lines at corners which are oriented perpendicular to each other into the same cluster. For each of these larger clusters, the orientation can now be determined with another PCA on the points of all road markings that are part of this cluster. All the rectangles in the cluster will then be oriented in the calculated direction.

5.2 Arrows

Arrows on the road are used to show which lane must be used for which direction at a crossing. There is only a relatively small number of arrows that are used in almost all situations, namely those pointing left, straight, right, and any combination of those. For this reason, templates of arrow shapes can be used. These templates are placed on the position where an arrow marking was found. The orientation is determined as best-fit in a way that they are covering the largest number of points of the detected road marking.

Using templates results in clearly shaped arrows in the result.

5.3 Other Markings

For other markings, such as barred areas and intersecting lines, the shapes have to be constructed in a different way. When the rectangle fitting described in Section 5.1 does not fit a marking or if the semantic type of the marking cannot be represented by rectangles or arrows, the following approach is used to generate a fitting shape.

A two-dimensional grid with squared cells with a side length of about 5 cm is created. The points of the respective marking are then placed into this grid. After all points have been added, each cell either contains points or not. Those cells containing points define the area that should be spanned by the created shape. The outline is generated by iterating over all outer cells at the border of the marking. For each cell, the outermost point will be used as a vertex for the generated polygon, resulting in a shape fitting closely to the detected road marking. The Douglas-Peucker algorithm (Douglas and Peucker, 1973) is used for shape simplification. Figure 7 shows some barred areas and crossing lines for which this approach was used.

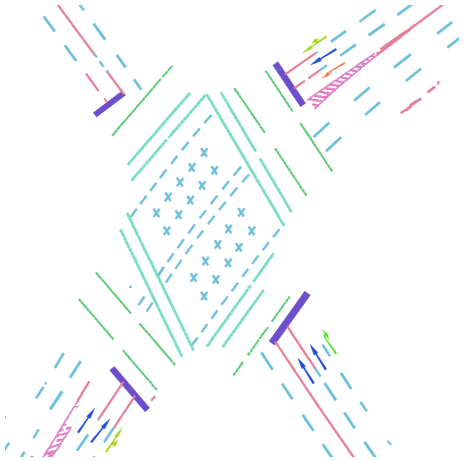

Figure 7: Automatically created shape file with shapes for individual road markings. Different colors represent different semantic classes.

6 EVALUATION

For the evaluation of the presented approach we used 3D point clouds which were recorded with the same hardware as the training data. They partly originate from the same cities as the training data and an additional city. Table 2 gives an overview of the data used. The artificial neural network was trained for 5 hours on a Nvidia GeForce 1080 Ti. In the manual evaluation 93.9 % of the road markings were correctly recognized, as shown in Table 3. The throughput was 7.5 million points per minute, which corresponds to about 300 meters of captured road per minute. The bottleneck in the analysis is the file operations during rendering, because a lot of data has to be written to disk. This could be avoided with an in-memory implementation.

Errors in the classification are mostly undetected road markings in areas of overall high intensity in wet regions of the road and wrongly assigned semantic classes like an incorrect type of line.

Table 3: Road marking accuracy values.

Marking	Prec.	Recall	F_1-score
Arrows (48)	93.5 %	89.6 %	91.5 %
Lane dividers (230)	96.6 %	98.7 %	97.7 %
Stop lines (39)	84.8 %	100.0 %	91.8 %
Ped. crossing (228)	91.2 %	97.0 %	94.0 %
Cycle tr. lines (270)	91.2 %	87.7 %	89.4 %
Barred areas (3)	100.0 %	100.0 %	100.0 %
Weighted average	92.5 %	93.9 %	93.1 %

The approach presented here achieves in our implementation comparable and partly even better results than the underlying procedure of Wen et al.

(2019) and the recently published capsule network-based approach of Ma et al. (2020). A full comparative evaluation with a larger dataset will be reflected in future work.

7 CONCLUSION AND FUTURE WORK

State-of-the-art 3D scanning technology allows to capture large-scale infrastructure networks (e. g., roads, railways) in unprecedented detail and precision. Due to their inherent quality these mobile mapping scans contain invaluable information for geospatial applications in areas such as urban planning and development, infrastructure management, predictive maintenance, and disaster management. As shown earlier, one such application is the automated identification and extraction of road markings, which allows for example to (1) improve and update pre-existing cadastre data and (2) check for erroneous or missing instances in an area. However, precisely identifying assets such as road markings in large-scale mobile mapping scans can be difficult and time-consuming.

We have shown that established artificial neural networks for image segmentation can be used to classify road markings in such 3D point cloud data sets efficiently and with great precision.

By choosing an appropriate rendering technique, detailed images of the captured ground are created, which can then be used as input for a neural network. It is possible to map the identified objects back into the 3D point cloud as well as to create shape files with the vector data which can be used in GIS applications. Depending on the type of road marking, different shape generation approaches are used for best results.

Besides road markings, the implementation can also be used to identify manhole covers and similar structures on the road, if labeled data sets with training data for the neural network are available. Similarly, our approach may be applied to railroad networks as a different mobile mapping area, allowing for the automated identification of rails, ties, and balises, as well as the extraction of generalized rail network plans which are essential for the maintenance and surveillance of such infrastructure.

In the future, we envision the ever increasing affordability of 3D scanning technology to result in scans being conducted more and more regular and by a larger variety of sensor systems, eventually leading to data sets that get updated every few minutes. The size of those data sets would dwarf that of today's scans, thus further necessitating the use of efficient classification approaches like the one detailed in this work.

ACKNOWLEDGMENTS

We thank the "Amt für Geoinformation, Vermessung und Kataster" of the city of Essen, Germany for provided data and insights into the requirements of road information analysis. Additionally we thank Ole Wegen for his contributions to this topic.

REFERENCES

Aringer, K. and Roschlaub, R. (2014). Bavarian 3d building model and update concept based on lidar, image matching and cadastre information. In *Innovations in 3D Geo-Information Sciences*, pages 143–157. Springer.

Bétaille, D. and Toledo-Moreo, R. (2010). Creating enhanced maps for lane-level vehicle navigation. *IEEE Transactions on Intelligent Transportation Systems*, 11(4):786–798.

Boulch, A., Saux, B. L., and Audebert, N. (2017). Unstructured point cloud semantic labeling using deep segmentation networks. In *Proceedings of 3DOR*, volume 2, page 1.

Caroti, G., Piemonte, A., and Pucci, B. (2005). Terrestrial laser scanning as road's cadastre revision and integration support. In *ISPRS Workshop Italy-Canada 2005 3D Digital Imaging and Modeling: Applications of Heritage, Industry*, volume 1, pages 1–3. CIRGEO.

Chen, D., Wang, R., and Peethambaran, J. (2017). Topologically aware building rooftop reconstruction from airborne laser scanning point clouds. *IEEE TGRS*, 55(12):7032–7052.

Douglas, D. H. and Peucker, T. K. (1973). Algorithms for the reduction of the number of points required to represent a digitized line or its caricature. *Cartographica: the international journal for geographic information and geovisualization*, 10(2):112–122.

ESRI (1998). Esri shapefile technical description. https://www.esri.com/library/whitepapers/pdfs/shapefile.pdf. Accessed: 2020-02-21.

Grilli, E., Menna, F., and Remondino, F. (2017). A review of point clouds segmentation and classification algorithms. *The International Archives of Photogrammetry, Remote Sensing and Spatial Information Sciences*, 42:339.

Guan, H., Li, J., Yu, Y., Wang, C., Chapman, M., and Yang, B. (2014). Using mobile laser scanning data for automated extraction of road markings. *ISPRS Journal of Photogrammetry and Remote Sensing*, 87:93–107.

Haala, N., Peter, M., Kremer, J., and Hunter, G. (2008). Mobile lidar mapping for 3d point cloud collection in urban areas—a performance test. *Int. Arch. Photogramm. Remote Sens. Spat. Inf. Sci*, 37:1119–1127.

Jaakkola, A., Hyyppä, J., Hyyppä, H., and Kukko, A. (2008). Retrieval algorithms for road surface modelling using laser-based mobile mapping. *Sensors*, 8:5238–5249.

LeCun, Y., Kavukcuoglu, K., and Farabet, C. (2010). Convolutional networks and applications in vision. In *Proceedings of 2010 IEEE international symposium on circuits and systems*, pages 253–256. IEEE.

Li, R. (1997). Mobile mapping: An emerging technology for spatial data acquisition. *Photogrammetric Engineering and Remote Sensing*, 63(9):1085–1092.

Ma, L., Li, Y., Li, J., Yu, Y., Junior, J. M., Gonçalves, W., and Chapman, M. (2020). Capsule-based networks for road marking extraction and classification from mobile lidar point clouds. *IEEE Transactions on Intelligent Transportation Systems*, pages 1–15.

Maurer, M., Gerdes, J. C., Lenz, B., Winner, H., et al. (2016). *Autonomous driving*. Springer, Berlin.

Meng, X., Wang, L., Silván-Cárdenas, J. L., and Currit, N. (2009). A multi-directional ground filtering algorithm for airborne lidar. *ISPRS Journal of Photogrammetry and Remote Sensing*, 64(1):117–124.

Mikrut, S., Kohut, P., Pyka, K., Tokarczyk, R., Barszcz, T., and Uhl, T. (2016). Mobile laser scanning systems for measuring the clearance gauge of railways: State of play, testing and outlook. *Sensors*, 16(5):683.

Niemeyer, J., Rottensteiner, F., and Soergel, U. (2012). Conditional random fields for lidar point cloud classification in complex urban areas. *ISPRS annals of the photogrammetry, remote sensing and spatial information sciences*, 1(3):263–268.

Pu, S., Rutzinger, M., Vosselman, G., and Elberink, S. O. (2011). Recognizing basic structures from mobile laser scanning data for road inventory studies. *ISPRS Journal of Photogrammetry and Remote Sensing*, 66(6):28–39.

Pulli, K., Baksheev, A., Kornyakov, K., and Eruhimov, V. (2012). Real-time computer vision with opencv. *Communications of the ACM*, 55(6):61–69.

Qi, C. R., Su, H., Mo, K., and Guibas, L. J. (2017). Pointnet: Deep learning on point sets for 3d classification and segmentation. In *Proceedings of the IEEE Conference on Computer Vision and Pattern Recognition*, pages 652–660.

Rabbani, T., Van Den Heuvel, F., and Vosselman, G. (2006). Segmentation of point clouds using smoothness constraint. *International Archives of Photogrammetry, Remote Sensing and Spatial Information Sciences*, 36(5):248–253.

Richter, R., Behrens, M., and Döllner, J. (2013). Object class segmentation of massive 3d point clouds of urban areas using point cloud topology. *International Journal of Remote Sensing*, 34(23):8408–8424.

Richter, R. and Döllner, J. (2013). Concepts and techniques for integration, analysis and visualization of massive 3D point clouds. *Computers, Environment and Urban Systems*, 45:114–124.

Ronneberger, O., Fischer, P., and Brox, T. (2015). U-net: Convolutional networks for biomedical image segmentation. In *International Conference on Medical image computing and computer-assisted intervention*, pages 234–241. Springer.

Schütz, M. and Wimmer, M. (2015). High-quality point-based rendering using fast single-pass interpolation. In *2015 Digital Heritage*, volume 1, pages 369–372. IEEE.

Schwalbe, E., Maas, H.-G., and Seidel, F. (2005). 3d building model generation from airborne laser scanner data using 2d gis data and orthogonal point cloud projections. *Proceedings of ISPRS WG III/3, III/4*, 3:12–14.

Vacek, S., Schimmel, C., and Dillmann, R. (2007). Road-marking analysis for autonomous vehicle guidance. In *EMCR*, pages 1–6.

Veit, T., Tarel, J.-P., Nicolle, P., and Charbonnier, P. (2008). Evaluation of road marking feature extraction. In *2008 11th International IEEE Conference on Intelligent Transportation Systems*, pages 174–181. IEEE.

Viola, P., Jones, M., et al. (2001). Rapid object detection using a boosted cascade of simple features. *CVPR (1)*, 1(511-518):3.

Vosselman, G., Dijkman, E., Reconstruction, K. W. B., Altimetry, L., and Transform, H. (2001). 3d building model reconstruction from point clouds and ground plans. *Int. Arch. of Photogrammetry and Remote Sensing*, XXXIV, Part 3/W4:37–43.

Vosselman, G., Gorte, B. G., Sithole, G., and Rabbani, T. (2004). Recognising structure in laser scanner point clouds. *International archives of photogrammetry, remote sensing and spatial information sciences*, 46(8):33–38.

Wen, C., Sun, X., Li, J., Wang, C., Guo, Y., and Habib, A. (2019). A deep learning framework for road marking extraction, classification and completion from mobile laser scanning point clouds. *ISPRS journal of photogrammetry and remote sensing*, 147:178–192.

Wolf, J., Richter, R., Discher, S., and Döllner, J. (2019a). Applicability of neural networks for image classification on object detection in mobile mapping 3d point clouds. *International Archives of the Photogrammetry, Remote Sensing & Spatial Information Sciences*, 42(4/W15):111–115.

Wolf, J., Richter, R., and Döllner, J. (2019b). Techniques for automated classification and segregation of mobile mapping 3d point clouds. In *Proceedings of the 14th International Joint Conference on Computer Vision, Imaging and Computer Graphics Theory and Applications*, pages 201–208.

Yang, B., Fang, L., Li, Q., and Li, J. (2012). Automated extraction of road markings from mobile lidar point clouds. *Photogrammetric Engineering & Remote Sensing*, 78(4):331–338.

Yu, Y., Li, J., Guan, H., Jia, F., and Wang, C. (2014). Learning hierarchical features for automated extraction of road markings from 3-d mobile lidar point clouds. *IEEE Journal of Selected Topics in Applied Earth Observations and Remote Sensing*, 8(2):709–726.

Zhang, Z., Liu, Q., and Wang, Y. (2018). Road extraction by deep residual u-net. *IEEE Geoscience and Remote Sensing Letters*, 15(5):749–753.

Zhou, Y. and Tuzel, O. (2018). Voxelnet: End-to-end learning for point cloud based 3d object detection. In *Proceedings of the IEEE Conference on Computer Vision and Pattern Recognition*, pages 4490–4499.